Design, Manufacturing and Testing of Magnetorheological Brake for Small Size Motorcycle

Conference Paper · January 2019

CITATIONS
0

READS
76

6 authors, including:

Thang Le-Duc
Vietnamese-German University
13 PUBLICATIONS **47** CITATIONS
SEE PROFILE

Nguyen Ngoc Diep
Posts and Telecommunications Institute of Technology
16 PUBLICATIONS **123** CITATIONS
SEE PROFILE

Enrique Duy
Pontificia Universidad Católica de Chile
2 PUBLICATIONS **0** CITATIONS
SEE PROFILE

Hung quoc Nguyen
Vietnamese-German University
114 PUBLICATIONS **1,398** CITATIONS
SEE PROFILE

Design, Manufacturing and Testing of Magnetorheological Brake for Small Size Motorcycle

LE Duc Thang[1, a], NGUYEN Ngoc Diep[2, b], LE Duy Tuan[2, c], NGUYEN Ngoc Tuyen[2, d], PHAM Van Vinh[2, e], NGUYEN Quoc Hung[1,*]

[1]Faculty of Engineering, Vietnamese-German University, Binh Duong, Viet Nam

[2]Industrial University of Ho Chi Minh City, HCM, Viet Nam

[a]thang.ld@vgu.edu.vn, [b]pdiep66@yahoo.com, [c]leduytuan1986@gmail.com, [d]nguyenngoctuyen@iuh.edu.vn, [e] phamvanvinh.tcnntn@gmail.com

*Corresponding author: Mail: hung.nq@vgu.edu.vn, Tel: (+84)938485812.

Keywords: Magneto-rheological Fluid (MRF); MR brake; motorcycle, optimal design

Abstract. In this research, a new type of magneto-rheological brake (MRB) is proposed for small size motorcycle. The proposed MRB consists of a rotor with multiple trapezoidal teeth acting at multiple magnetic poles of the brake. In order to generate a magnetic field for controlling braking torque, a magnetic coil is placed on each side-housing of the brake. The inner face of each side-housing also has trapezoidal shape mating with the trapezoidal teeth of the rotor via MRF layer. By applying countercurrents to the coils, a magnetic fluid is generated with some magnetic flux going across the MRF layer (MRF duct) between the rotor teeth and their mating poles on the housing. By using multiple poles with trapezoidal shape, a high braking torque of the brake is expected while the size of the brake is still kept to be compacted. After an introduction about the development of MRBs in automotive engineering, the configuration of the proposed MRB is presented and its braking torque is derived based on Bingham rheological model of MRF. The proposed MRB is then optimally designed based on finite element analysis (FEA). Its optimized MRB is then manufactured and its braking performance is experimentally investigated. The MRB is then installed in a prototype motorcycle and the field test of this prototype motorcycle integrated with the MRB is then conducted.

Introduction

In the past two decades, some studies in development and application of smart brake featuring magneto-rheological fluid (MRF) have attracted the attention of many researchers. The application for automotive vehicles or motorcycles is an interesting field in design MRB. Some researches on improving the performance of MRB for the above applications can be listed here. Park *et al.* [1] investigated a magneto-rheological brake design which is operated via a sliding-mode controller. Karakoc *et al.* [2] proposed the design considerations for building a feasible automotive MRB. Nguyen *et al.* [3] performed an optimal design of different disc-type MRBs considering the geometric volume and the off-state temperature constraints. After that, Nguyen *et al.* [4] proposed a hybrid MRB configuration for motorcycles which considered the radial and axial magnetic flux in order to increase its braking force and simultaneously decrease its mass. Although all abovementioned literature shows the high potential abilities of MRBs in automotive and motorcycle applications, the experimental results on examining their actual performance are still lacked. Recently, Nguyen *et al.* [5] designed a new MRB in which two magnetic coils is fixed on both sides of the MRB housings (in this work, it is called as double side-coil MRB). The optimal results showed that some disadvantages of the traditional ones such as the "bottle-neck" problem of magnetic flux, the nonmagnetic bobbin are required, and the difficulties in manufacturing and maintenance can be eliminated or minimized by using this configuration. In addition, the optimal solutions also performed that in providing the same braking torque, the mass of the double side-coil MRB was significantly improved in comparison with the conventional ones. Nevertheless, all of abovementioned MRB configurations just consider the disc which has the simple rectangular shape. Thus, in this study, the rotor which has a more complex profile created by many trapezoids is considered to apply to a typical MRB. Its MRB with a rotor having multiple trapezoidal teeth and multiple coils placed on the side housings is expected to provide the significantly better performance than the previous ones in the literature.

The remainder of the paper is displayed as follows. Section 2 shows the proposed multiple trapezoidal-teeth MRB with two coils placed on the side housings and some equations for estimating its braking torque. Section 3 presents the optimal design problem and the optimization procedure for the proposed MRB. Results and discussions are then described in section 4. Finally, some conclusions are performed in section 5.

The multiple trapezoidal-teeth MR brake with coils placed on the side housings

A configuration of an MRB with a rotor having multiple trapezoidal teeth and two coils placed on the side housing (in this research, it named as the multiple trapezoidal-teeth side-coil MRB) is proposed. Fig. 1a displays a typical double side-coil MRB and Fig. 1b presents the multiple trapezoidal-teeth side-coil one. Each abovementioned MRB has a disc (rotor) made of magnetic steel is fixed to the flange of the shaft made by nonmagnetic steel. The disc is also covered by a stationary envelope (housing) made of magnetic steel. In both two configurations, the coils are placed directly on side housing of the brake. As countercurrents are applied to the coils, a mutual magnetic field is generated to produce the braking force. It can be seen that the profile of the rotor and the inner housings in the case of the double side-coil MRB are rectangular while the respective ones in the case of the proposed MRB are made by some continuous trapezoidal contours. This trapezoidal-teeth profile makes the contact surface between the MRF and the disc increase; thereby, the induced braking torque of the multiple trapezoidal-teeth side-coil MRB is expected to increase notably.

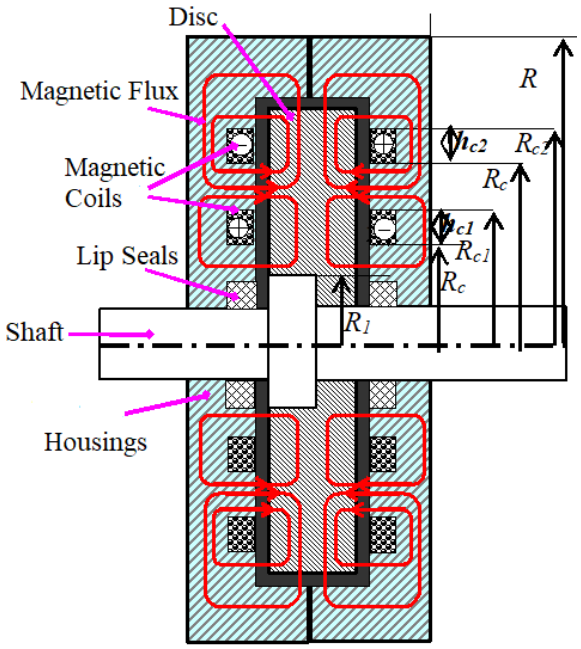

(a) The double side-coil MRB

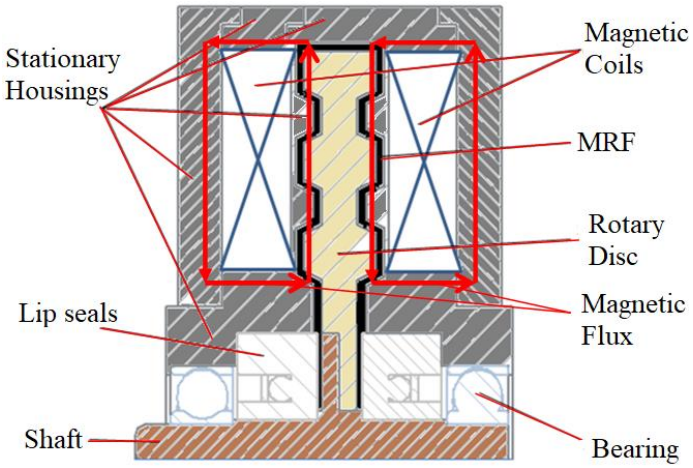

(b) The multiple trapezoidal-teeth side-coil MRB

Figure 1. Configurations of the double side-coil and the multiple trapezoidal-teeth side-coil MRBs

In order to calculate braking torque generated by the MRB, a small ring element in the inclined MRF gap as displayed in Fig. 2 is considered. The friction torque applied to this element can be evaluated as:

$$dT = r\tau \mathrm{d}A = 2\pi r^2 \tau \mathrm{d}l = 2\pi(R_1 + l\sin\varphi)^2 \tau \mathrm{d}l \tag{1}$$

Where r is the radius of the sloping small ring element with respect to the rotation axis of the MRB; R_1 and R_2 are respectively the radius calculated from the first end and the last end of the slope gap with respect to the rotation axis; L_a is the projected length of the slope gap with respect to the rotation axis; φ is the angle between the slope gap and the rotation axis; l is the length of the slope gap. In addition, the shear rate of MRF in the duct can be approximated as:

$$\dot{\gamma} = \frac{r\Omega}{d} \tag{2}$$

where Ω is the angular velocity of the disc.

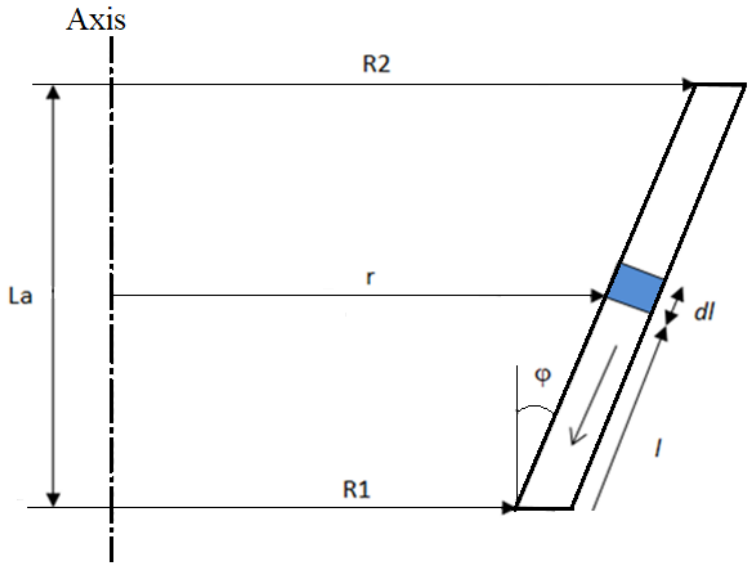

Figure 2. Annular ring element of MR fluid in the slope duct

The Bingham model of MRF along the axial direction can be expressed as:

$$\tau = \tau_y + \mu\frac{r\Omega}{d} = \tau_y + \mu\frac{\Omega(R_1+l\sin\varphi)}{d} \tag{3}$$

where τ is the shear stress acting on the MRF; τ_y and μ_0 are respectively the zero-field yield stress and the viscosity of the MRF. Replacing some variables defined by Eqs. (2) – (3) to the corresponding ones in Eq. (1), the following equation is gained:

$$T = 2\pi\int_0^{L_a/cos\varphi}(R_1+lsin\varphi)^2\tau d = 2\pi\int_0^{l}(R_1+lsin\varphi)^2\left(\tau_y+\mu\frac{\Omega(R_1+l\sin\varphi)}{d}\right)d$$

$$= 2\pi\left(R_1^2l + R_1l^2sin\varphi + \frac{1}{3}l^3sin^2\varphi\right)\tau_y + \frac{1}{2}\pi\mu\frac{l\Omega}{d}(4R_1^3 + 6R_1^2lsin\varphi + 4R_1l^2sin^2\varphi + l^3sin^3\varphi) \tag{4}$$

Fig. 3 shows the description for the division of the MRF ducts in order to estimate the total braking torque of MRB. The total braking torque is generated into three different kinds of the MRF ducts including the inclined gaps A1, A2, A3, A4 and A5, the annular gap C1 and the radial end-face gaps E1, E2, E3, E4, E5, and E6. Based on Eqs. (4) , the induced partial braking torque generated into each MRF duct can be estimated as follows:

$$T_{ve1} = \frac{\pi\mu_{e1}R_1^4}{2d}[1-(\frac{R_i}{R_1})^4]\Omega + \frac{2\pi\tau_{ye1}}{3}(R_1^3-R_i^3) \tag{5}$$

$$T_{ve2} = \frac{\pi\mu_{e2}R_3^4}{2d}[1-(\frac{R_2}{R_3})^4]\Omega + \frac{2\pi\tau_{ye2}}{3}(R_3^3-R_2^3) \tag{6}$$

$$T_{ve3} = \frac{\pi\mu_{e3}R_5^4}{2d}[1-(\frac{R_4}{R_5})^4]\Omega + \frac{2\pi\tau_{ye3}}{3}(R_5^3-R_4^3) \tag{7}$$

$$T_{ve4} = \frac{\pi\mu_{e4}R_7^4}{2d}[1-(\frac{R_6}{R_7})^4]\Omega + \frac{2\pi\tau_{ye4}}{3}(R_7^3-R_6^3) \tag{8}$$

$$T_{ve5} = \frac{\pi\mu_{e5}R_9^4}{2d}[1-(\frac{R_8}{R_9})^4]\Omega + \frac{2\pi\tau_{ye5}}{3}(R_9^3-R_8^3) \tag{9}$$

$$T_{ve6} = \frac{\pi\mu_{e6}R_d^4}{2d}[1-(\frac{R_{10}}{R_d})^4]\Omega + \frac{2\pi\tau_{ye6}}{3}(R_d^3-R_{10}^3) \tag{10}$$

$$\begin{aligned} T_{a1} &= 2\pi(R_1^2 l + R_1 l^2 \sin\varphi + \frac{1}{3}l^3\sin^2\varphi)\tau_{ya1} \\ &+ \frac{1}{2}\pi\mu_{a1}\frac{\pi}{d}(4R_1^3 + 6R_1^2 l\sin\varphi + 4R_1 l^2\sin^2\varphi + l^3\sin^3\varphi) \end{aligned} \tag{11}$$

$$\begin{aligned} T_{a2} &= 2\pi(R_3^2 l + R_3 l^2 \sin\varphi + \frac{1}{3}l^3\sin^2\varphi)\tau_{ya2} \\ &+ \frac{1}{2}\pi_{a2}\mu\frac{\pi}{d}(4R_3^3 + 6R_3^2 l\sin\varphi + 4R_3 l^2\sin^2\varphi + l^3\sin^3\varphi) \end{aligned} \tag{12}$$

$$\begin{aligned} T_{a3} &= 2\pi(R_5^2 l + R_5 l^2 \sin\varphi + \frac{1}{3}l^3\sin^2\varphi)\tau_{ya3} \\ &+ \frac{1}{2}\pi\mu_{a3}\frac{\pi}{d}(4R_5^3 + 6R_5^2 l\sin\varphi + 4R_5 l^2\sin^2\varphi + l^3\sin^3\varphi) \end{aligned} \tag{13}$$

$$\begin{aligned} T_{a4} &= 2\pi(R_7^2 l + R_7 l^2 \sin\varphi + \frac{1}{3}l^3\sin^2\varphi)\tau_{ya4} \\ &+ \frac{1}{2}\pi\mu_{a4}\frac{\pi}{d}(4R_7^3 + 6R_7^2 l\sin\varphi + 4R_7 l^2\sin^2\varphi + l^3\sin^3\varphi) \end{aligned} \tag{14}$$

$$\begin{aligned} T_{a5} &= 2\pi(R_9^2 l + R_9 l^2 \sin\varphi + \frac{1}{3}l^3\sin^2\varphi)\tau_{ya5} \\ &+ \frac{1}{2}\pi\mu_{a5}\frac{\pi}{d}(4R_9^3 + 6R_9^2 l\sin\varphi + 4R_9 l^2\sin^2\varphi + l^3\sin^3\varphi) \end{aligned} \tag{15}$$

$$T_{c1} = 2\pi R_d^2(b+2hh)(\tau_{yc1} + \mu_{c1}\frac{\Omega R_d}{d}) \tag{16}$$

The total braking torque is expressed by:

$$T_b = 2(T_{ve1}+T_{ve2}+T_{ve3}+T_{ve4}+T_{ve5}+T_{ve6}+T_{a1}+T_{a2}+T_{a3}+T_{a4}+T_{a5}) + T_{c1} + 2T_s \tag{17}$$

where T_s is the lip seal friction force which can be approximately evaluated by [6]

$$T_s = (f_c L_c + f_h A_r)R_s \tag{18}$$

In the above equation, T_s is the friction torque of a lip seal acting on the shaft of the MRB, f_c is the friction force per unit length of the shaft perimeter due to O-ring compression depending on the percentage of seal compression and the hardness of the O-ring material, L_c is the friction length of the inner face of the lip seals (shaft perimeter), f_h is the O-ring friction based on the fluid pressure applying to a unit projected area of the brake shaft, A_r is the seal projected area and R_s is the shaft diameter at the sealing.

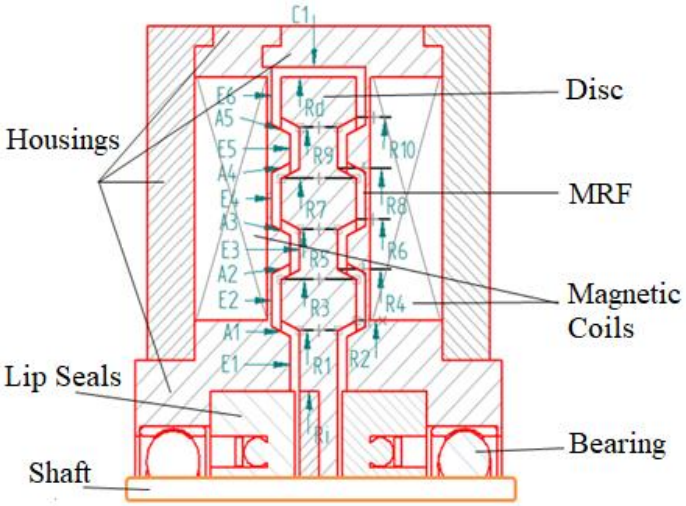

Figure 3. The division of MRF ducts for evaluating the braking torque

Optimal design of the proposed MRB

In this section, the optimization problem of the multiple trapezoidal-teeth, the double and the triple side-coil MRBs is considered for the small-sized motorcycles. It is noteworthy that the braking torque and the mass of MRBs are two important factors which their objectives are opposite. In detail, an MRB structure should be as small as possible in providing a required braking torque for minimizing its size and cost [5,8]. Therefore, in this paper, the objective of the MRB optimal design is to find the lightest MRB structure which can produce a critical braking torque for a determined small-sized motorcycle. Generally, the optimal design of MRBs can be expressed as [5,6,8]

$$\text{Minimize} \quad m_b = V_d\rho_d + V_h\rho_h + V_s\rho_s + V_{MR}\rho_{MR} + V_c\rho_c \tag{19}$$

$$\text{Subject to} \quad x_i^L \le x_i \le x_i^U,\ i = 1, 2 \ldots n$$

$$[T_0] \le T_b$$

where V_d, V_h, V_s, V_{MR}, V_{bob}, and V_c are the volume of the disc, the housing, the shaft, the MRF, the bobbin and the coil of the brake, respectively; ρ_d, ρ_h, ρ_s, ρ_{MR}, ρ_{bob} and ρ_c are the density of the discs, the housing, the shaft, the MRF and the coil material, correspondingly; x_i^L and x_i^U are the lower and upper bounds of the corresponding geometric dimensions of MRBs; n is the number of design variables; $[T_0]$ and T_b are respectively the required and the induced braking torque of the MRBs for a predetermined small-sized motorcycle.

This section shows the optimal results of all abovementioned MRBs and some relative discussions are performed in detail. The magnetic components (the housing and the disc) of the MRB are made by the commercial steel C45. The MRF used in this study is MRF132-DG and its rheological parameters obtained by using curve fitting method from experimental results are shown as: $\mu_0 = 0.1pa \cdot s$; $\mu_\infty = 3.8pa \cdot s$; $\alpha_{s\mu} = 4.5T^{-1}$; $\tau_{y0} = 15pa$; $\tau_{y\infty} = 40000\,pa$; $\alpha_{st_y} = 2.9T^{-1}$. The size of copper coil wires is 24-gage (diameter = 0.511mm) and its maximum working current is around 3A. However, in this research, a current of 2.5A is applied to the coil to investigate the MRB performance. In the optimal design problem, some important geometric dimensions of the MRBs such as the coil height (h_c, h_{cj}), the coil width (w_c, w_{cj}), the inner radius R_i and outer radius R_d of the MRF duct, the disc thickness t_d, outer radius of the brake R, the housing thickness t_h and the inner radius of the coils R_{ci} are considered as design variables. The required braking torque is 150Nm [4].

Table 1 shows the optimal solutions of the MRBs. In this table, it can be seen that the mass of the multiple trapezoidal-teeth side-coil MRB is significantly smaller than the double side-coil MRB.

In detail, the optimal mass of the proposed MRB is 4.55kg while the ones of the double side-coil MRB is 12.47kg. In addition, the coil resistance in the case of the multiple trapezoidal-teeth side-coil MRB is the lowest (12.6Ω for the multiple trapezoidal-teeth side-coil MRB; 15.3Ω for the double side-coil MRBs); therefore, its power consumption is also smaller. Fig. 4 shows magnetic density distribution of the MRBs at their optimal configurations. It is observed that the magnetic distribution in the housing of the multiple trapezoidal-teeth side-coil MRB is more uniformed than that of two remaining ones.

Table 1 Optimal solution of the MRBs when the required torque is 150Nm

MRB types	Design parameter [mm]	Characteristics
Trapezoidal-teeth side-coil MRB	**Coil:** Width w_c=*7.7*; Height h_c,=24; No. of turns: 493 **Housing:** R_s=30, R=68.5, t_h=5, L=36.3 **Disc:** Radius R_i=32.5, R_d=63.5; Thickness t_d= 4.8 **MRF duct gap**: 1.0	**Max. Torque:** 150.06 [Nm] **Mass:** 4.55 [kg] **Total Coil Resistance:** R_c=12.6 [Ω]
Double side-coil MRB	**Coil:** Width $w_{c1} = w_{c2}$=*6.7*; Height h_{c1} =10; h_{c2}=8.7; No. of turns: 180 + 156 = 336 **Housing:** R_s=30, R=118.9, t_h=12.5, L=37.1 **Disc:** Radius R_i=32.5, R_d=116.4; Thickness t_d= 10.6 **MRF duct gap**: 1.0	**Max. Torque:** 150.42 [Nm] **Mass:** 12.47 [kg] **Total Coil Resistance:** R_c = 6.7 + 8.6 = 15.3 [Ω]

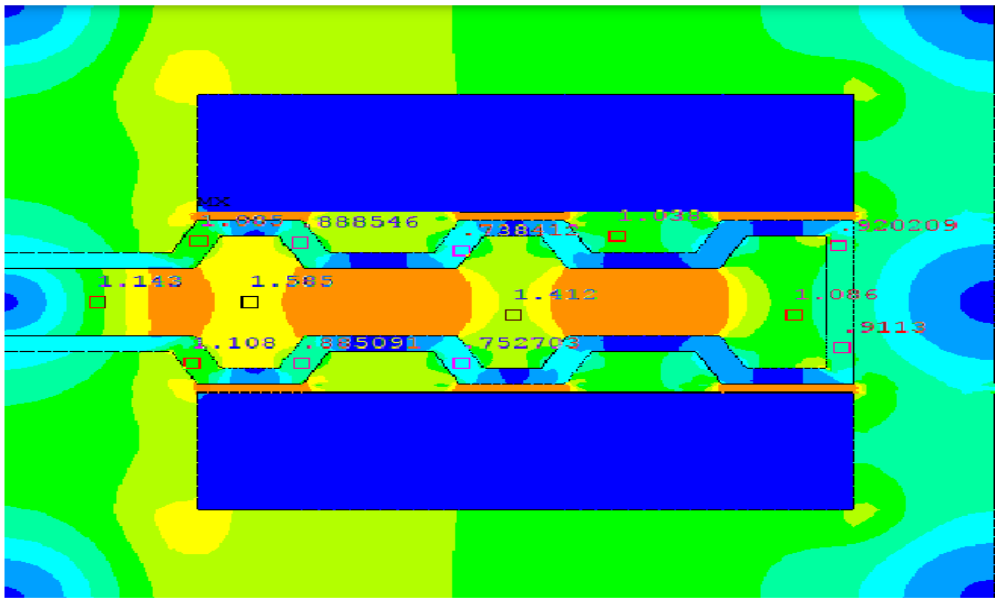

(a) The proposed MRB

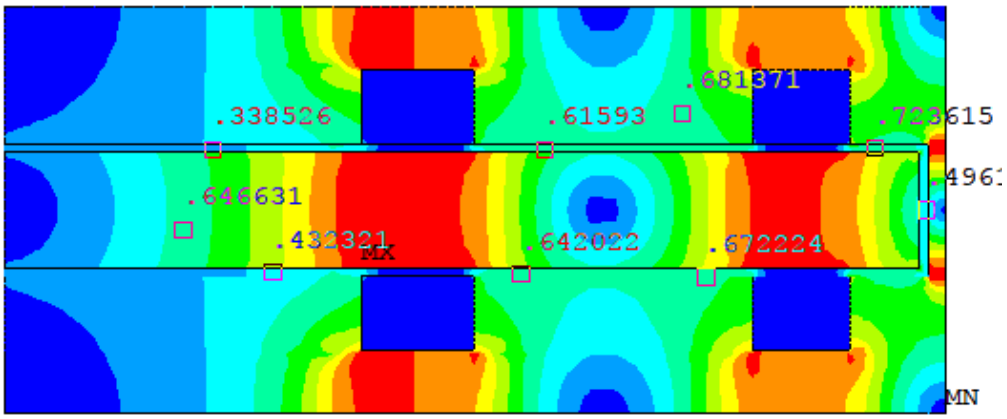

(b) The double side-coil MRB

Figure 4. Magnetic flux density of the brakes at the optimum

Experimental results

To validate the precision of all above optimal results, the experiments should be performed to examine their actual performance. In this study, the prototype of the proposed MRB is manufactured based on the results which are shown in Table 1. The major parts of the prototype are shown in Fig. 5.

The experimental setup for testing the performance of the prototype is proposed in Fig. 6. A gear-box DC motor revolving the shaft of the MRB rotor at a constant angular speed of 19π *rad/s*. A force sensor is used to measure the acting load generated by the MRB. The analog output signal from the force sensor is then sent to the computer for evaluation. When the experiment process is stated, step current signals from the computer are transferred to the current amplifier. Various currents from 0A to 2.5A with a step of 0.25A are finally applied to the coils of the proposed MRB to create the braking forces.

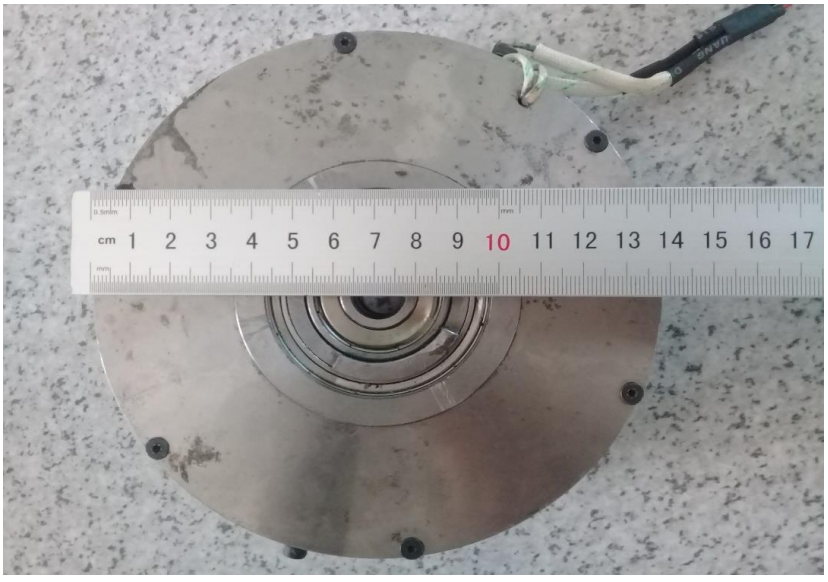

Figure 5. prototype of the multiple trapezoidal-teeth side-coil MRB for experimental testing

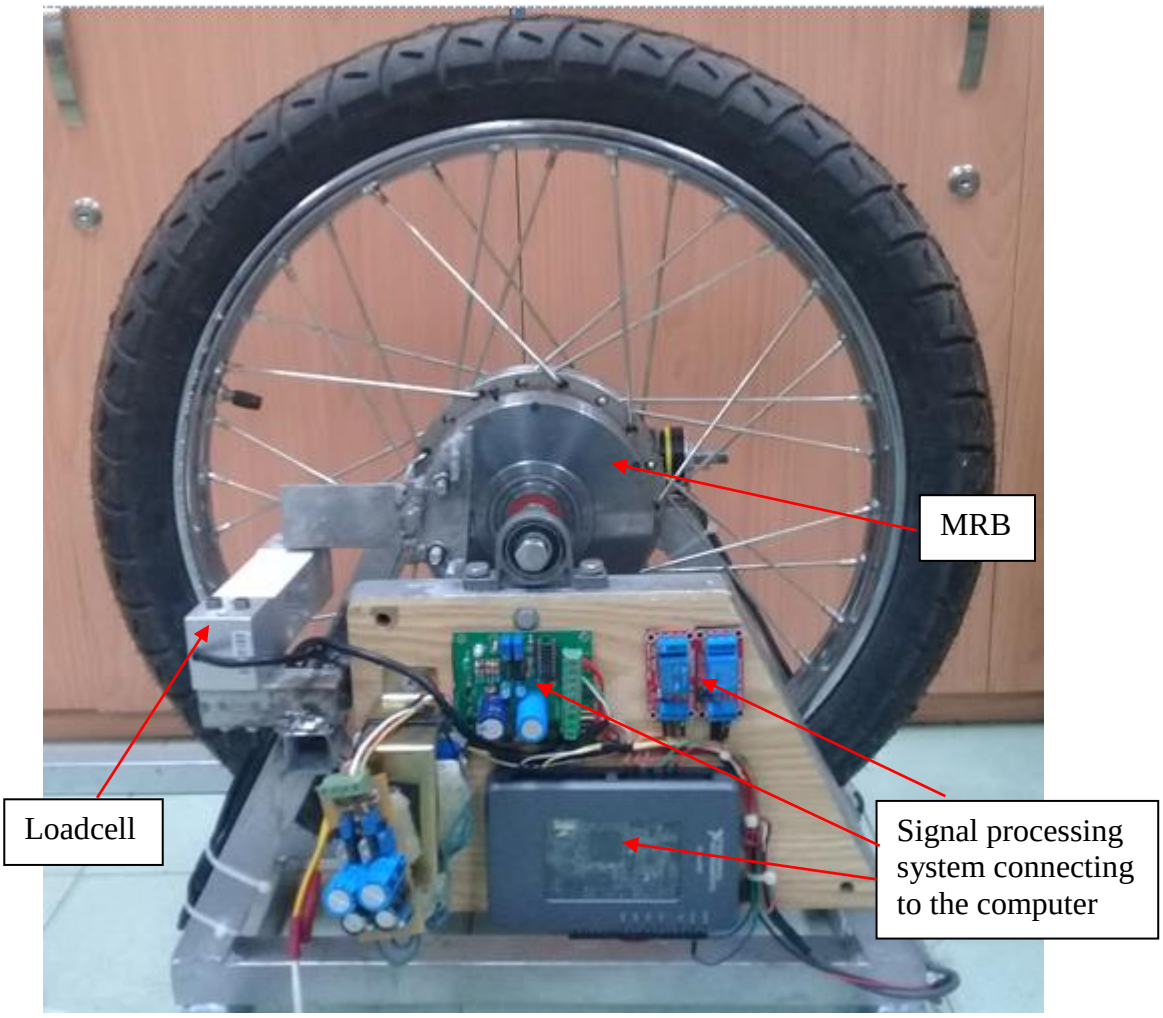

Figure 6. Experiment setup to test the performance of the prototype of proposed MRB

Fig. 7 shows step response of the multiple trapezoidal-teeth side-coil MRB prototypes at the step time of 0.5 sec with various currents from 0A to 2.5A being applied to the coils. It is realized that the response time of the induced braking torque also tends to increase with respect to the growth of the values of the applied currents. In detail, the response times in the cases of the current magnitude of 0.5A and 1A are respectively 0.3s and 0.4s; while those in the remaining cases are above 0.5s. In addition, the higher the current magnitude is, the greater the average value of torque will be. Fig. 8 shows braking torque of the MRB as a function of the applied current. The results show quite good agreement between the simulated and experimental results. The errors of the braking torque between the simulation and the experiment is around 11%. This error is mainly come from the coil filling ratio of the prototype, the loss of magnetic field to the ambient and at the contact between the magnetic parts of the MRBs. In addition, inaccurate estimation of the proposed MRBs can be also a potential reason.

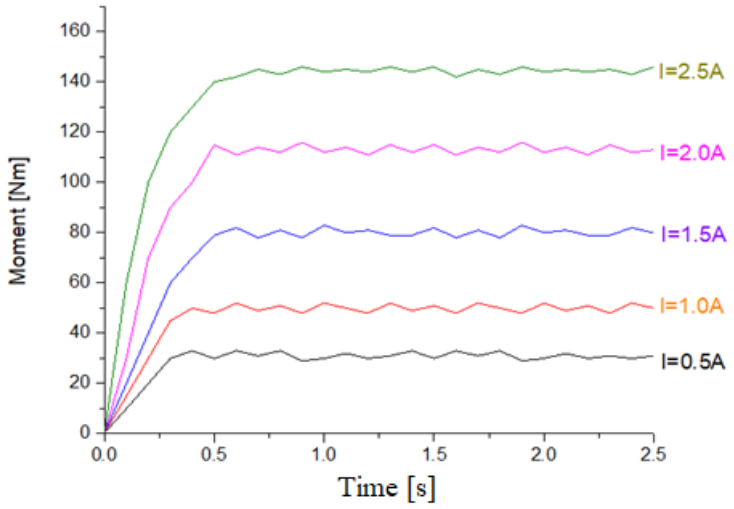

Figure 7. Step response of the proposed MRB

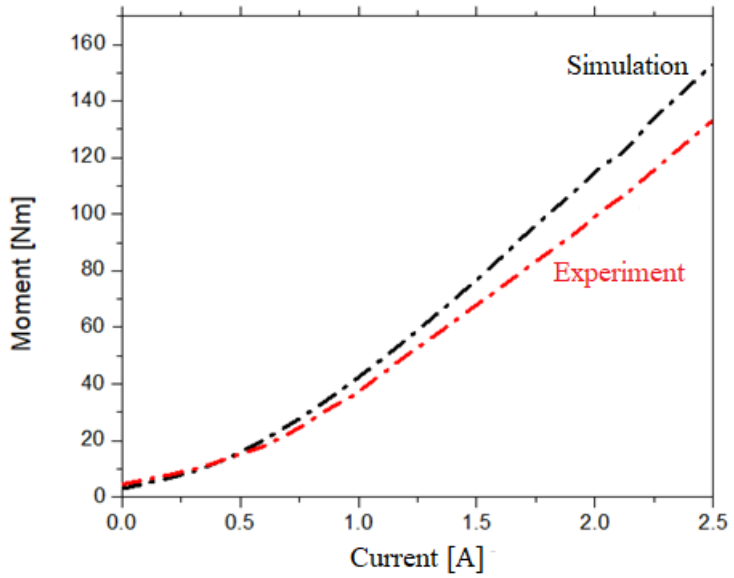

Figure 8. The braking torque of the proposed MRB as a function of the applied current magnitude

Conclusions

In this work, the MR brake with a rotor having multiple trapezoidal teeth and two coils placed on both side housings, which was referred as multiple trapezoidal-teeth side-coil MRB, was proposed and evaluated for the small-sized motorcycle application. Based on Bingham rheological model of the MR fluid, the braking torque of the proposed MRB was derived analytically. After that, the optimization procedure of three considered MRBs involving the multiple trapezoidal-teeth and the double side-coil was performed based on magnetic FEA module in ANSYS software. The optimal results showed that with the same braking torque constraint, the multiple trapezoidal-teeth side-coil MRB is significantly lighter than the double side-coil MRB. Moreover, the coil resistance in the case of the proposed MRB is also notably smaller which results in lower power consumption. Experimental solutions on the proposed MRB showed that the errors of the achieved braking torque between the analytical results and the experimental ones is around 11%, which agreed quite well with each others. As second phase of this research, a field test of the proposed MRB is conducted and heating, durability of the proposed MRB are considered.

Acknowledgement

This work was supported by the Vietnam National Foundation for Science and Technology Development (NAFOSTED) under grant no. 107.01-2016.32.

References

[1] E.J. Park, D. Stoikov, L. Falcao da Luz, A. Suleman, A performance evaluation of an automotive magnetorheological brake design with a sliding mode controller, Mechatronics **16** (2006) 405–416

[2] K. Karakoc, E. J. Park, A. Suleman, Design considerations for an automotive magnetorheological brake, Mechatronics **18** (2008) 434–47

[3] Q. H. Nguyen, S. B. Choi, Optimal design of an automotive magnetorheological brake considering geometric dimensions and zero-field friction heat, *Smart Materials and Structures* **19** (2010) 115024

[4] Q. H. Nguyen, S. B. Choi, Optimal design of a novel hybrid MR brake for motorcycles considering axial and radial magnetic flux, Smart Materials and Structures **21** (2012) 55003

[5] Q. H. Nguyen, N. D. Nguyen, S. B. Choi, Design and evaluation of a novel MR brake with coils placed on side housings, Smart Materials and Structures **24** (2015) 90590I

[6] Q. H.Nguyen, V. T. Lang, N. D. Nguyen, S. B. Choi, Geometric optimal design of a magneto-rheological brake considering different shapes for the brake envelope, Smart Materials and Structures **23** (2014) 15020

[7] M. Zubieta, S. Eceolaza, M. J. Elejabarrieta, M. M. Bou-Ali, Magnetorheological fluids: characterization and modeling of magnetization, Smart Materials and Structures **18** (2009) 95019

[8] D. T. Le, H. V. Ho, T. T. Nguyen and Q. H. Nguyen, A new design approach based on differential evolution algorithm for geometric optimization of magnetorheological brakes, Smart Materials and Structures **25** (2016) 125020

[9] Q. H. Nguyen, S. B. Choi, Optimal design of a vehicle magnetorheological damper considering the damping force and dynamic range, Smart Materials and Structures **18** (2009) 15013

[10] Q. H. Nguyen, Y. M. Han, S. B. Choi and N. M. Wereley, Geometry optimization of MR valves constrained in a specific volume using the finite element method *Smart Materials and Structures* **16** (2007) 2242–52